



DI-HIGGS PRODUCTION VIA AXION-LIKE PARTICLES



Collaborators: Fabian Esser, Maeve Madigan, Verónica Sanz and Maria Ubiali.

8th Red LHC workshop, Thursday 30th May, 2024

Alexandre Salas-Bernárdez

8th Red LHC Workshop

28 – 30 May 2024 @ U. Complutense (Madrid)

Outline

- 1 Introduction and motivation.

Outline

- 1 Introduction and motivation.
- 2 Di-Higgs in the chiral ALP.

Outline

- 1 Introduction and motivation.
- 2 Di-Higgs in the chiral ALP.
- 3 ALP contribution to di-Higgs in the $b\bar{b}\gamma\gamma$ final state.

Outline

- 1 Introduction and motivation.
- 2 Di-Higgs in the chiral ALP.
- 3 ALP contribution to di-Higgs in the $b\bar{b}\gamma\gamma$ final state.
- 4 A smoking gun for the ALP-mediated di-Higgs production.

Outline

- 1 Introduction and motivation.
- 2 Di-Higgs in the chiral ALP.
- 3 ALP contribution to di-Higgs in the $b\bar{b}\gamma\gamma$ final state.
- 4 A smoking gun for the ALP-mediated di-Higgs production.
- 5 ALP-mediated di-Higgs from top loops.

Outline

- 1 Introduction and motivation.
- 2 Di-Higgs in the chiral ALP.
- 3 ALP contribution to di-Higgs in the $b\bar{b}\gamma\gamma$ final state.
- 4 A smoking gun for the ALP-mediated di-Higgs production.
- 5 ALP-mediated di-Higgs from top loops.

Based on *“Di-Higgs production via Axion-Like Particles”*,
[2404.08062](#)

Introduction

Alexandre Salas-Bernárdez

Axion-Like Particles for BSM physics

BSM phenomena to be explained

- Dark matter.

Axion-Like Particles for BSM physics

BSM phenomena to be explained

- Dark matter. Dark energy.

Axion-Like Particles for BSM physics

BSM phenomena to be explained

- Dark matter. Dark energy.
- Matter-antimatter asymmetry.

Axion-Like Particles for BSM physics

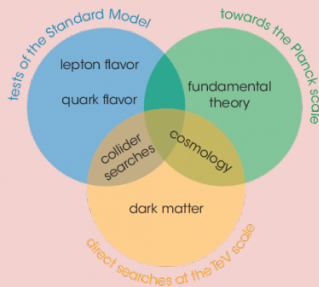
BSM phenomena to be explained

- Dark matter. Dark energy.
- Matter-antimatter asymmetry.
- Neutrino masses.

Axion-Like Particles for BSM physics

BSM phenomena to be explained

- Dark matter. Dark energy.
- Matter-antimatter asymmetry.
- Neutrino masses.
- ...



ALPs are strong candidates for SM extensions:

- Introduced for solving the strong CP problem (?).
- ALPs appear in scenarios of global symmetry breaking in new confining sectors (pNGB).

Di-Higgs in the chiral ALP

Alexandre Salas-Bernárdez

Linear vs. chiral ALP: linear (SMEFT-like) 1701.05379

Linear ALP theory (expansion in terms of the inverse of the ALP scale f_a). Dimension-five interactions with the SM gauge fields,

$$\mathcal{L} \supset -\frac{a}{f_a} \left(c_{\tilde{B}} B_{\mu\nu} \tilde{B}^{\mu\nu} + c_{\tilde{W}} W_{\mu\nu}^a \tilde{W}^{a,\mu\nu} + c_{\tilde{G}} G_{\mu\nu}^a \tilde{G}^{a,\mu\nu} \right) .$$

Linear vs. chiral ALP: linear (SMEFT-like) 1701.05379

Linear ALP theory (expansion in terms of the inverse of the ALP scale f_a). Dimension-five interactions with the SM gauge fields,

$$\mathcal{L} \supset -\frac{a}{f_a} \left(c_{\tilde{B}} B_{\mu\nu} \tilde{B}^{\mu\nu} + c_{\tilde{W}} W_{\mu\nu}^a \tilde{W}^{a,\mu\nu} + c_{\tilde{G}} G_{\mu\nu}^a \tilde{G}^{a,\mu\nu} \right) .$$

Coupling to the Higgs doublet, H ,

$$\mathcal{O}_{aH} = i \left(H^\dagger \overleftrightarrow{D}_\mu H \right) \frac{\partial^\mu a}{f_a} ,$$

Linear vs. chiral ALP: linear (SMEFT-like) 1701.05379

Linear ALP theory (expansion in terms of the inverse of the ALP scale f_a). Dimension-five interactions with the SM gauge fields,

$$\mathcal{L} \supset -\frac{a}{f_a} \left(c_{\tilde{B}} B_{\mu\nu} \tilde{B}^{\mu\nu} + c_{\tilde{W}} W_{\mu\nu}^a \tilde{W}^{a,\mu\nu} + c_{\tilde{G}} G_{\mu\nu}^a \tilde{G}^{a,\mu\nu} \right) .$$

Coupling to the Higgs doublet, H ,

$$\mathcal{O}_{aH} = i \left(H^\dagger \overleftrightarrow{D}_\mu H \right) \frac{\partial^\mu a}{f_a} ,$$

which leads to fermionic couplings proportional to the Yukawas,

$$\mathcal{O}_{a\psi} = i \frac{a}{f_a} (\bar{Q}_L Y_U \tilde{H} u_R + \dots) + h.c.$$

Linear vs. chiral ALP: chiral (HEFT-like) 1701.05379

We find 17 possibilities for coupling the ALP to SM fields,

$$\mathcal{L}_{\text{chiral}} = \sum_{i=\tilde{B}, \tilde{W}, \tilde{G}} c_i \mathcal{O}_i + \sum_{j=1}^{17} c_j \mathcal{O}_j,$$

Linear vs. chiral ALP: chiral (HEFT-like) 1701.05379

We find 17 possibilities for coupling the ALP to SM fields,

$$\mathcal{L}_{\text{chiral}} = \sum_{i=\vec{B}, \vec{W}, \vec{G}} c_i \mathcal{O}_i + \sum_{j=1}^{17} c_j \mathcal{O}_j,$$

where each of the operators $\mathcal{O}_1 - \mathcal{O}_{17}$ is proportional to a Higgs flare function (see J. Martinez-Martín's talk) such as

$$\mathcal{F}_i(h) = 1 + a_i \frac{h}{v} + b_i \left(\frac{h}{v} \right)^2 + \dots,$$

New couplings: c_{2D} , which induces $Z^\mu \partial_\mu a$.

Other relevant operators: such as the operator c_{17} which accompanies $\frac{1}{f_a} V_\mu \partial^\mu \square a$.

Linear vs. chiral ALP: chiral (HEFT-like) 1701.05379

We find 17 possibilities for coupling the ALP to SM fields,

$$\mathcal{L}_{\text{chiral}} = \sum_{i=\vec{B}, \vec{W}, \vec{G}} c_i \mathcal{O}_i + \sum_{j=1}^{17} c_j \mathcal{O}_j,$$

where each of the operators $\mathcal{O}_1 - \mathcal{O}_{17}$ is proportional to a Higgs flare function (see J. Martinez-Martín's talk) such as

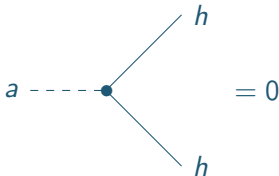
$$\mathcal{F}_i(h) = 1 + a_i \frac{h}{v} + b_i \left(\frac{h}{v} \right)^2 + \dots,$$

New couplings: c_{2D} , which induces $Z^\mu \partial_\mu a$.

Other relevant operators: such as the operator c_{17} which accompanies $\frac{1}{f_a} V_\mu \partial^\mu \square a$.

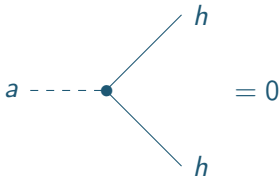
CP conserving ALP interactions

ALPs are pseudoscalar particles (0^-).



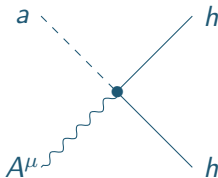
CP conserving ALP interactions

ALPs are pseudoscalar particles (0^-).



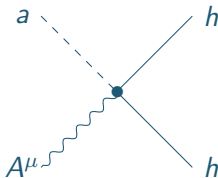
⇒ Need for an extra γ or Z boson.

CP conserving ALP interactions



$$\frac{1}{2\pi v^2 f_a} \left(\tilde{b}_3 c_W + \tilde{b}_{10} s_W \right) (p_\gamma^\mu p_a^2 - p_\gamma^2 p_a^\mu) \stackrel{\text{on shell}}{=} 0$$

CP conserving ALP interactions



$$\frac{1}{2\pi v^2 f_a} \left(\tilde{b}_3 c_W + \tilde{b}_{10} s_W \right) (p_\gamma^\mu p_a^2 - p_\gamma^2 p_a^\mu) \stackrel{\text{on shell}}{=} 0$$

This is due to CP conservation \Rightarrow
 $0^- \longrightarrow 0^-$ which needs **longitudinal polarization** of outgoing
 vector boson.

Process of this analysis

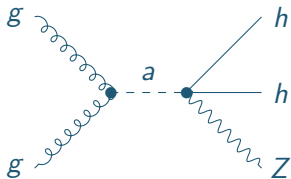
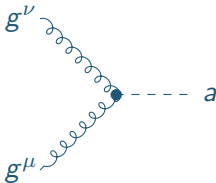
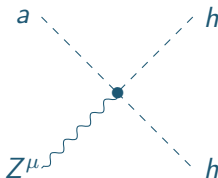


Figure 1: Feynman diagram for di-Higgs production with an associated Z-boson via a non-resonant ALP.

ALP from gg fusion

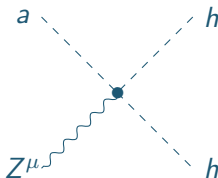
$$-\frac{4i}{f_a} c_{\tilde{G}} p_{g1\alpha} p_{g2\beta} \varepsilon^{\mu\nu\alpha\beta}$$

Di-Higgs from ALP



$$\frac{g}{4\pi^2 c_W v^2 f_a} \left[p_{hh}^\mu (p_a^2 \tilde{b}_{11} + p_a \cdot p_{hh} \tilde{b}_{14}) + p_a^\mu (p_{hh}^2 \tilde{b}_{13} + p_a \cdot p_{hh} \tilde{b}_{12}) \right. \\ \left. + 2\tilde{a}_{16} (p_{h1}^\mu p_a \cdot p_{h2} + p_{h2}^\mu p_a \cdot p_{h1}) + 4\tilde{a}_{15} p_a^\mu p_{h1} \cdot p_{h2} \right. \\ \left. - p_a^\mu (16\pi^2 v^2 \tilde{b}_{2D} - \tilde{b}_{17} p_a^2) + 2\pi s_{2W} \tilde{b}_{310} (p_Z^2 p_a^\mu - p_Z^\mu p_a \cdot p_Z) / e \right]$$

Di-Higgs from ALP



$$\frac{g}{4\pi^2 c_W v^2 f_a} \left[p_{hh}^\mu (p_a^2 \tilde{b}_{11} + p_a \cdot p_{hh} \tilde{b}_{14}) + p_a^\mu (p_{hh}^2 \tilde{b}_{13} + p_a \cdot p_{hh} \tilde{b}_{12}) \right. \\ \left. + 2\tilde{a}_{16} (p_{h1}^\mu p_a \cdot p_{h2} + p_{h2}^\mu p_a \cdot p_{h1}) + 4\tilde{a}_{15} p_a^\mu p_{h1} \cdot p_{h2} \right. \\ \left. - p_a^\mu (16\pi^2 v^2 \tilde{b}_{2D} - \tilde{b}_{17} p_a^2) + 2\pi s_{2W} \tilde{b}_{310} (p_Z^2 p_a^\mu - p_Z^\mu p_a \cdot p_Z) / e \right]$$

Many structures! We choose 3 relevant Benchmarks.

Benchmarks of this analysis

Benchmark 1: $\tilde{b}_{3,10-17} = \tilde{a}_{15,16} = \tilde{b}_{2D} = 1$,

Benchmark 2: $\tilde{b}_{2D} = 1$, all others set to zero,

Benchmark 3: $\tilde{b}_{17} = 1$, all others set to zero.

ALP to di-Higgs in $b\bar{b}\gamma\gamma$

Alexandre Salas-Bernárdez

ATLAS analysis: [2310.12301](#)

Up to date there is no search with HHZ final state.

ATLAS analysis: 2310.12301

Up to date there is no search with HHZ final state.

We can use ATLAS analysis when the Z remains invisible.

$$pp \rightarrow hh + X \rightarrow b\bar{b}\gamma\gamma + X ,$$

ATLAS analysis: 2310.12301

Up to date there is no search with HHZ final state.

We can use ATLAS analysis when the Z remains invisible.

$$pp \rightarrow hh + X \rightarrow b\bar{b}\gamma\gamma + X ,$$

We take the ALP-mediated production of two Higgses in this final state $b\bar{b}\gamma\gamma$ plus a Z boson decaying to neutrinos or jets.

ATLAS analysis: 2310.12301

Up to date there is no search with HHZ final state.

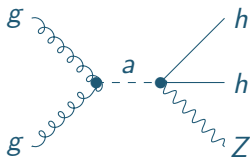
We can use ATLAS analysis when the Z remains invisible.

$$pp \rightarrow hh + X \rightarrow b\bar{b}\gamma\gamma + X ,$$

We take the ALP-mediated production of two Higgses in this final state $b\bar{b}\gamma\gamma$ plus a Z boson decaying to neutrinos or jets.

ATLAS does not place explicit vetoes on missing energy, and the veto on additional jets is quite lax.

Limits from ATLAS data



We will denote the combination of gluon and electroweak bosons with the letter c , namely

$$c \equiv c_{\tilde{G}} c_{3B} ,$$

The partonic cross section scales as

$$\hat{\sigma}(gg \rightarrow a \rightarrow hhZ) \propto \hat{s}^3 \frac{c_{\tilde{G}}^2 c_{3B}^2}{v^4 f_a^4} .$$

Limits from ATLAS data

We now compare the total number of measured events (n_{obs}) to the background estimate provided by ATLAS n_{BG} , and our signal prediction n_{s} , which depends on the combination c/f_a^2 .

Limits from ATLAS data

We now compare the total number of measured events (n_{obs}) to the background estimate provided by ATLAS n_{BG} , and our signal prediction n_s , which depends on the combination c/f_a^2 . We perform a χ^2 test

$$\chi^2 \left(\frac{c}{f_a^2} \right) = \left(\frac{n_{\text{obs}} - n_{\text{BG}} - n_s(c/f_a^2)}{\Delta_{\text{BG}}} \right)^2,$$

where Δ_{BG} denotes the quadratic sum of the background uncertainties as provided by ATLAS.

Limits from ATLAS data

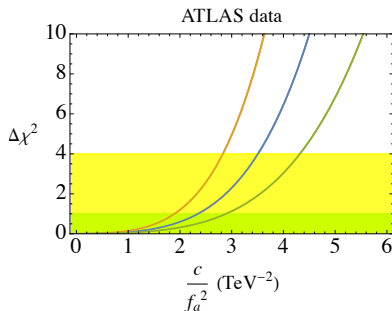


Figure 2: Dependence of $\Delta\chi^2$ on c/f_a^2 . Benchmark 1 (blue line), Benchmark 2 (orange line) and Benchmark 3 (green line).

The limits corresponding to 2 standard deviations translate into

$$f_a > (0.53, 0.59, 0.48) \times \sqrt{c} \text{ TeV}$$

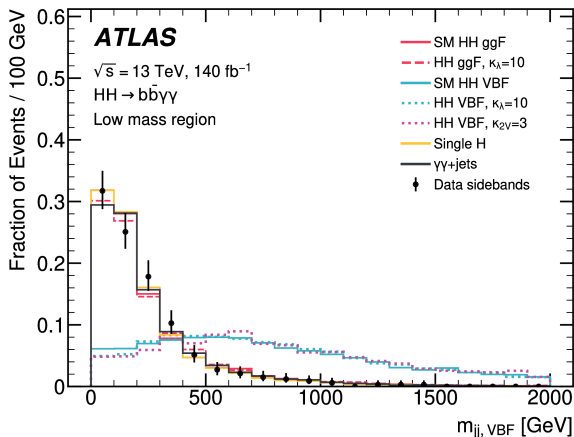
for Benchmark 1, Benchmark 2 and Benchmark 3, respectively.

ALP-mediated di-Higgs differential distributions

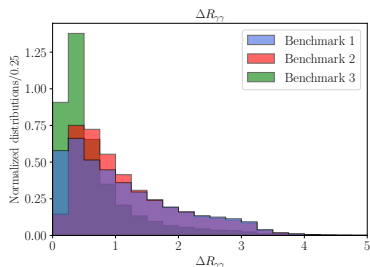
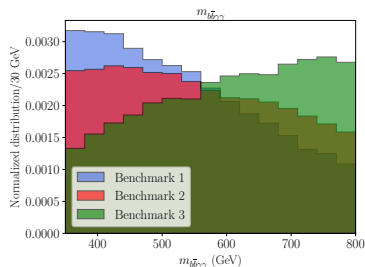
ATLAS analysis has differential distributions normalized to one and focused on regions defined by BDT classifiers, leaving insufficient details for comparing our signal events with the observed data.

ALP-mediated di-Higgs differential distributions

ATLAS analysis has differential distributions normalized to one and focused on regions defined by BDT classifiers, leaving insufficient details for comparing our signal events with the observed data.

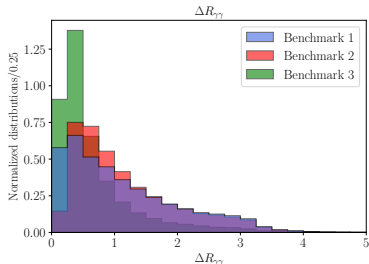
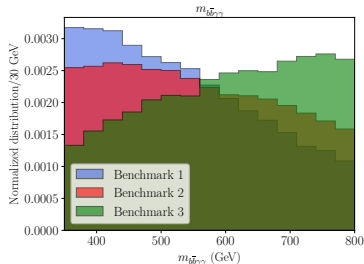


Differential Distributions



Products of ALPs are highly collimated! (contrary to SM signal).
Accessing the ATLAS distributions would greatly improve the analysis.

Differential Distributions



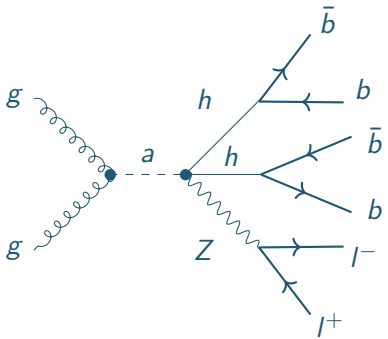
Products of ALPs are highly collimated! (contrary to SM signal). Accessing the ATLAS distributions would greatly improve the analysis.

In contrast to the EFT case (κ_{2V} modifier) analyzed by ATLAS, the ALP-mediated signal does not exhibit interference with the SM di-Higgs production.

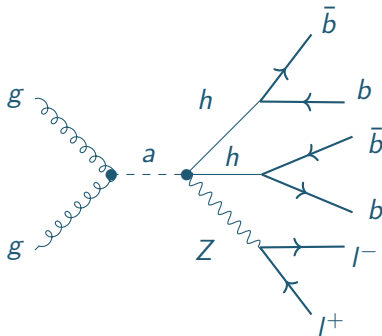
A smoking gun for ALP to di-Higgs

Alexandre Salas-Bernárdez

Dedicated search

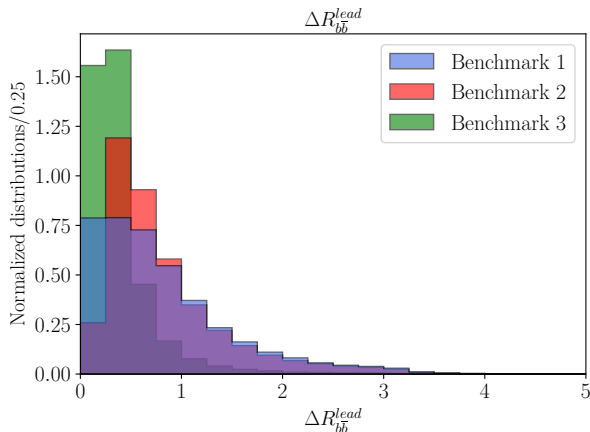


Dedicated search

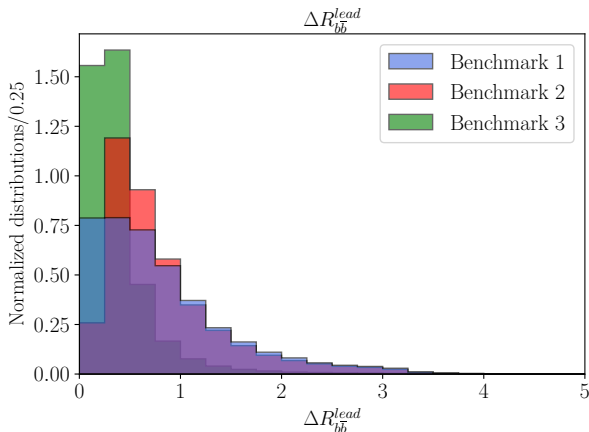


Need to estimate SM background with the relevant cuts.

Differential Distributions

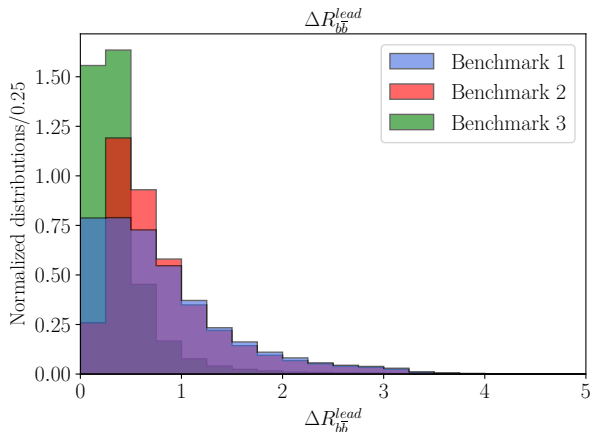


Differential Distributions



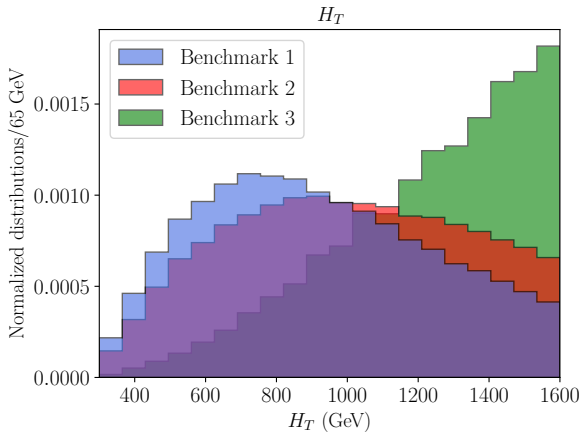
Highly collimated bs from the leading Higgs,

Differential Distributions

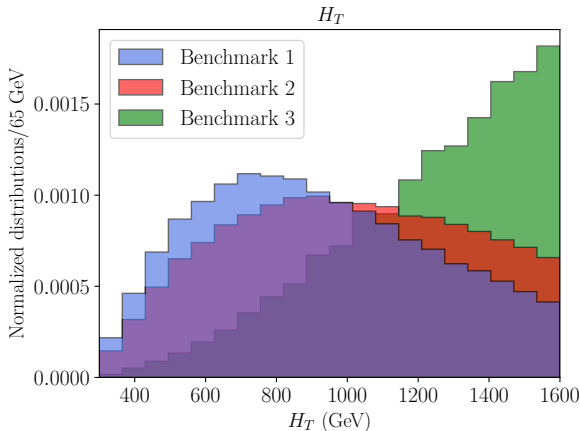


Highly collimated b s from the leading Higgs,
 \Rightarrow non isolation of b jets in many cases (fat jets).

Differential Distributions



Differential Distributions



Cut $H_T > 500$ GeV, with good acceptance.

SM Background of $gg \rightarrow hhZ \rightarrow Z + 4b$ jets

Removing the isolation condition, the cross section would increase to 7 fb.

SM Background of $gg \rightarrow hhZ \rightarrow Z + 4b$ jets

Removing the isolation condition, the cross section would increase to 7 fb. However, the merging of b-jets would result in a different final state topology.

SM Background of $gg \rightarrow hhZ \rightarrow Z + 4b$ jets

Removing the isolation condition, the cross section would increase to 7 fb. However, the merging of b -jets would result in a different final state topology.

In [1303.6636](#) the authors propose a tagging algorithm for two Higgses into b -jets which could go from the fully resolved 4 b final state, to intermediate fat jet + 2 b -jets situation, and reaching the two fat jet case (around 50% efficiency across all channels).

SM Background of $gg \rightarrow hhZ \rightarrow Z + 4b$ jets

Removing the isolation condition, the cross section would increase to 7 fb. However, the merging of b -jets would result in a different final state topology.

In [1303.6636](#) the authors propose a tagging algorithm for two Higgses into b -jets which could go from the fully resolved 4 b final state, to intermediate fat jet + 2 b -jets situation, and reaching the two fat jet case (around 50% efficiency across all channels).

Mistagging quarks is heavily suppressed.

SM Background of $gg \rightarrow hhZ \rightarrow Z + 4b$ jets

Removing the isolation condition, the cross section would increase to 7 fb. However, the merging of b -jets would result in a different final state topology.

In [1303.6636](#) the authors propose a tagging algorithm for two Higgses into b -jets which could go from the fully resolved 4 b final state, to intermediate fat jet + 2 b -jets situation, and reaching the two fat jet case (around 50% efficiency across all channels).

Mistagging quarks is heavily suppressed.

Finally, applying an additional cut on $H_T > 500$ GeV brings the cross section from 4 to around 2 fb.

Sensitivity estimate

We can assess the potential sensitivity of a dedicated analysis using Run 2 LHC data.

The typical cross section of the signal is

$$\sigma(pp \rightarrow hhZ)_{ALP} \simeq \left(\frac{c}{f_a^2 (\text{TeV})} \right)^2 (230 - 530) \text{ fb} .$$

Sensitivity estimate

We can assess the potential sensitivity of a dedicated analysis using Run 2 LHC data.

The typical cross section of the signal is

$$\sigma(pp \rightarrow hhZ)_{ALP} \simeq \left(\frac{c}{f_a^2 (\text{TeV})} \right)^2 (230 - 530) \text{ fb} .$$

Comparing (Signal S vs Background B) this with the 2 fb cross section from the SM,

$$\frac{S}{\sqrt{B}} \simeq \frac{\sigma_{ALP} \text{Br}(h \rightarrow b\bar{b})^2 \sqrt{\text{Br}(Z \rightarrow 2\ell)}}{\sqrt{\sigma_{SM}}} \epsilon_b^2 \sqrt{\mathcal{L}} ,$$

Sensitivity estimate

We can assess the potential sensitivity of a dedicated analysis using Run 2 LHC data.

The typical cross section of the signal is

$$\sigma(pp \rightarrow hhZ)_{ALP} \simeq \left(\frac{c}{f_a^2 (\text{TeV})} \right)^2 (230 - 530) \text{ fb} .$$

Comparing (Signal S vs Background B) this with the 2 fb cross section from the SM,

$$\frac{S}{\sqrt{B}} \simeq \frac{\sigma_{ALP} \text{Br}(h \rightarrow b\bar{b})^2 \sqrt{\text{Br}(Z \rightarrow 2\ell)}}{\sqrt{\sigma_{SM}}} \epsilon_b^2 \sqrt{\mathcal{L}} ,$$

which produces a ($S/\sqrt{B} = 2$, 95% C.L) limit on the size of of ALP-mediated contribution

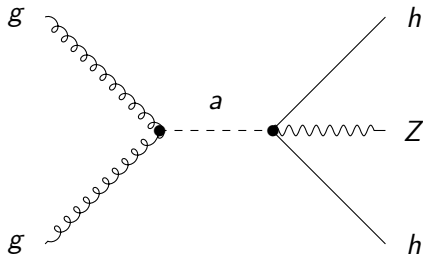
$$f_a \gtrsim 2.4\text{-}3.0 \times \sqrt{c} \text{ TeV}$$

which much more sensitive.

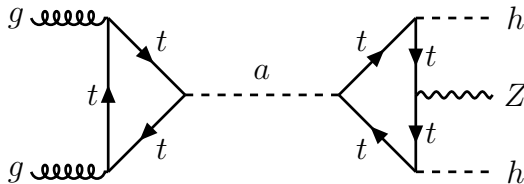
Linear ALP to di-Higgs through top loops

Alexandre Salas-Bernárdez

Comparing to linear theory

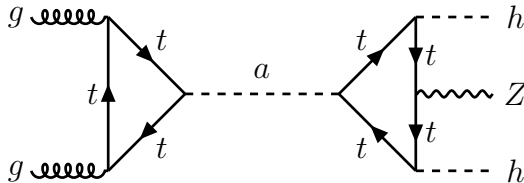


Comparing to linear theory: top loops



$$\mathcal{L} = -i c_t \frac{m_t a}{f_a} (\bar{t} \gamma^5 t)$$

Comparing to linear theory: top loops

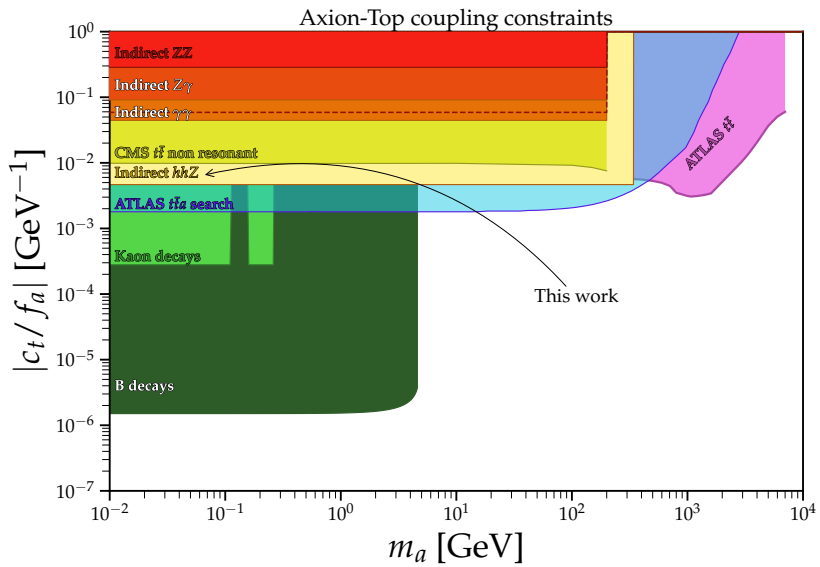


$$\mathcal{L} = -i c_t \frac{m_t a}{f_a} (\bar{t} \gamma^5 t)$$

Using Naive Dimensional Analysis (NDA) we can interpret the results from the last section in terms of loop contributions as

$$\frac{c}{f_a^2} \simeq \frac{\alpha_s}{8\pi c_W} \frac{c_t^2}{f_a^2}.$$

Bounds on top-axion couplings



Conclusions

- Di-Higgs production from ALPs needs an extra vector boson.

Conclusions

- Di-Higgs production from ALPs needs an extra vector boson.
- Sensitivity would increase if ATLAS or CMS data and DD is made accessible.

Conclusions

- Di-Higgs production from ALPs needs an extra vector boson.
- Sensitivity would increase if ATLAS or CMS data and DD is made accessible.
- A dedicated search (f.e. HHZ) can place very strong limits on ALP couplings to Higgses.

Conclusions

- Di-Higgs production from ALPs needs an extra vector boson.
- Sensitivity would increase if ATLAS or CMS data and DD is made accessible.
- A dedicated search (f.e. HHZ) can place very strong limits on ALP couplings to Higgses.
- Results can be translated to the linear-ALP theory, placing competitive bounds.

Aknowledgments

Support from the EU's Next Generation funding, grant number CNS2022-135688.

Funded by research grant PID2022-137003NB-I00 from spanish MCIN/AEI/10.13039/501100011033/ and EU FEDER.

This work has been supported in part by Spanish MICINN (PID2022-137003NB-I00, PID2021-124473NB-I00, PID2019-108655GB-I00/AEI/10.13039/501100011033), U. Complutense de Madrid under research group 910309, the IPARCOS institute, the EU under grant 824093 (STRONG2020).